DSTO

Analysis of Fatigue Crack Growth from Cold-expanded/interference Fitted Stop Drilled Holes

R.J. Callinan, C.H. Wang and S. Sanderson

DSTO-TR-0704

APPROVED FOR PUBLIC RELEASE

DEPARTMENT OF DEFENCE
DEFENCE SCIENCE AND TECHNOLOGY ORGANISATION

Analysis of Fatigue Growth from Cold-expanded/interference Fitted Stop Drilled Holes

R.J.Callinan, C.H.Wang and S.Sanderson

Airframes and Engines Division
Aeronautical and Maritime Research Laboratory

DSTO-TR-0704

ABSTRACT

In this report a numerical study has been carried out into the fatigue life enhancement of a through cracked plate specimen using stop drilled holes at the end of each crack tip. Also the effect of cold working and the use of interference plugs are considered. While it has been found that under a static remote tension load the use of interference plugs gives no additional static strength, results from cyclic loads indicate that the accumulation of strain energy per cycle is less with interference fit plugs. Also the introduction of stationary cracks of crack-length *0.066* to *1.0mm* have been considered with constraints to prevent crack closure. The crack-tip opening displacements of re-initiated cracks at the edge of the stop hole have been determined using the finite element method, and it is found that the equivalent stress intensity factors are significantly higher than predicted by linear elastic fracture mechanics. Furthermore the use of these results together with the FASTRAN II computer program predicts fatigue lifetimes which are in reasonable agreement with experimental data.

DEPARTMENT OF DEFENCE

DEFENCE SCIENCE AND TECHNOLOGY ORGANISATION

Published by

DSTO Aeronautical and Maritime Research Laboratory
PO Box 4331
Melbourne Victoria 3001

Telephone: (03) 9626 7000
Fax: (03) 9626 7999

AR-010-604
July 1998

APPROVED FOR PUBLIC RELEASE

Analysis of Fatigue Crack Growth from Cold-expanded/interference Fitted Stop Drilled Holes

Executive Summary

When fatigue cracks are found in aircraft structures the safe life of the structure is of concern. If the fatigue life can be safely extended then aircraft operating costs can be lowered. Previous work has found that plastic expansion of a hole resulting in residual compression upon elastic recovery can result in a decrease of the mean stress under cyclic loads resulting both in an increase of life and an increased critical crack length. In an experimental program recently carried out at AMRL a procedure was used to stop drill the crack, cold work the stop hole and use interference fit plugs. This resulted in an increase of stress level by a factor of 2 for fatigue life of 10,000 Falstaff blocks.

In this report a theoretical investigation is carried out into the fatigue life enhancement of a cracked plate specimen using a combination of stop drilling, cold expansion and interference fitting. Firstly the stress/strain state in the area in which cracks re-initiate from the cold worked hole is analysed using the ABAQUS finite element program. This involves an elastic-plastic and non-linear contact analysis. Validation of this work has been carried out using closed form solutions for plugs in holes for an infinite plate, corresponding to (1) cold expansion, (2) removal of the mandrel, (3) insertion of an interference plug, and (4) application of a remote load. It has been found that in the absence of an applied remote load the residual stress distribution in the area in which cracks would develop is approximately the same as would be expected in a cold expanded hole in an infinite plate. Also it has been found that under static tension loads use of cold working and interference plugs gives no additional strength, however results obtained from cycling of loads indicate that accumulation of strain energy per cycle is considerably less for cold worked and interference fit plugs, and hence a considerable improvement in life would be expected. Secondly, the introduction of short stationary cracks of crack-length of *0.066* to *1.0mm* has been considered with constraints to prevent crack closure. The crack-tip opening displacements of re-initiated cracks at the edge of the stop hole have been determined using the finite element method, and it is found the equivalent stress intensity factors are significantly higher than those obtained by linear elastic fracture mechanics. From these results together with the FASTRAN II computer program, fatigue lifetimes are predicted which are in reasonable agreement with experimental data for these specimens.

Overall it has been found that the combination of interference fit plugs with cold expansion of the stop drilled holes significantly reduce the crack driving force and hence extends the fatigue life of a cracked structure. Results achieved in this report indicate that this is a promising procedure for the life extension of RAAF aircraft structures.

Authors

R.J.Callinan
Airframes and Engines Division

Mr. R.J.Callinan is a senior research scientist and graduated from RMIT (Aero. Eng.) in 1969 and from Monash University in 1971 (Civil. Eng.) and completed a M.Eng. Sc. in 1981 at Melbourne University. His work has been in the areas of finite element analysis, fracture mechanics and structural mechanics of composite and bonded repairs, and military aircraft accident investigations. He has also been involved with design studies of low radar cross-section battlefield surveillance R.P.V.'s. In 1985 he was seconded to the USAF at Eglin AFB for 18 months, to carry out vulnerability studies on composite structures. More recently he has been involved in a specific program on validation of bonded repairs to RAAF aicracft, and bonded repairs subject to acoustic fatigue.

C.H.Wang
Airframes and Engines Division

Dr. Chun Wang joined DSTO in 1995 as a Senior Research Scientist. After completing his Ph.D in 1990 at the University of Sheffield, UK, Dr. Wang since has held various academic positions at Deakin University, the University of Sydney and the University of Sheffield, UK, prior to joining DSTO. His research interests include fatigue and fracture mechanics, bonded joints and repairs, advanced composite materials, constitutive modelling and cracking of Macadamia nuts.

S.Sanderson
Airframes and Engines Division

Mr. Sanderson has worked at AMRL since 1981. He has developed flight data reduction & analysis software for Mirage, F-111 & F/A-18 projects. Several of these programs have been implemented by NAE for their data reduction in the IFOST project. Since 1992 Mr.Sanderson has been involved with the F.E. analysis of composite and bonded structures for F-111 & F/A-18.

Contents

SYMBOLS

1. INTRODUCTION 1

2. ANALYSIS 2
2.1 Step 1: cold-expansion of stop-hole 3
2.2 Step 2: removal of expansion mandrel 3
2.3 Step 3: insertion of interference plug 4

3. FINITE ELEMENT ANALYSIS OF COLD-EXPANSION OF A STOP-HOLE 5
3.1 Step 1: cold-expansion 5
3.2 Step 2: removal of mandrel 5
3.3 Step 3: Insertion of interference plug 6

4. APPLICATION OF REMOTE LOAD TO COMBINED INTERFERENCE FITTING AND COLD-EXPANSION OF STOP-HOLES 8

5. STRESS ANALYSIS: INTERFERENCE PLUG SUBJECT TO CYCLIC LOAD 10
5.1 Tangential stress and load level 10
5.2 Stress/strain curves 12

6. COMPUTATION OF STRESS INTENSITY FACTOR OF RE-INITIATED CRACK 15
6.1 Analytical approach 15
6.2 Method for computation of stress intensity factors 17
6.3 Discussion on analytical and F.E. analysis 18
6.4 Fatigue life prediction 21

7. CONCLUSIONS 23

8. REFERENCES 24

APPENDIX: METHOD FOR COMPUTATION OF STRESS INTENSITY FACTORS 26

Symbols

α	material constant
α	also denotes the constraint factor
ε	strain
ε_0	yield strain
δ_T	crack tip opening displacement
λ	interference
θ	angle
σ	stress
σ_θ	tangential stress
σ_r	radial stress
σ_z	stress perpendicular to plate
σ_0	yield stress
ρ	radius to re-yielded zone
ν	poisson's ratio
ν_m	poisson's ratio for mandrel
ΔK_{eff}	effective stress intensity factor
ΔK_{th}	threshold stress intensity factor
a_1	re-initiated crack-length
$2a_o$	length of long crack
C	material constant
CTOD	crack tip opening displacement
E	Young's modulus of aluminium
E_m	Young's modulus of mandrel
d_n	displacement variable
$G(a_1,r)$	stress intensity of a crack a_1 due to point force at distance r
I_n	variable
J	J integral
K	stress intensity factor
K_p	plastic stress intensity factor
c	radius to elastic-plastic boundary
m	work hardening exponent
n	work hardening exponent
p	interference pressure
R	hole radius
r	radius
u_x	x displacement near crack tip
u_y	y displacement near crack tip

1. Introduction

As a result of high acquisition costs of aircraft, life enhancement techniques are being increasingly used to reduce overall operating costs. Generally the growth of fatigue cracks determine the safe life of the structure. Life enhancement techniques involving removal of cracks in fastener holes and fitting interference inserts are well known. However experimental work carried out by (Finney et al ,1996) has found that the fatigue lifetime of a cracked plate specimen in which the crack tips have been stop drilled and cold expanded is also considerably enhanced. The geometry of the cracked plate is shown in Figure 1. The crack has a length of $2.a_o = 20mm$ and is referred to as the long crack. Numerical and experimental work has also been carried out by (Vulic 1997) for cracks emanating from a single hole in which a mandrel is used to cold work the hole. However the aim of this report is to understand the mechanism by which the fatigue life is enhanced. An investigation is carried out into the stress state when the hole is: (1) cold expanded, (2) the mandrel is removed, (3) the insertion of an interference plug and (4) subject to a remote applied load. The interference (λ) is defined as the ratio of the difference in hole diameters between the hole and mandrel to the diameter of the hole. In the work carried out here the interference level for cold expansion is 4% and interference for the plugs is .67%.

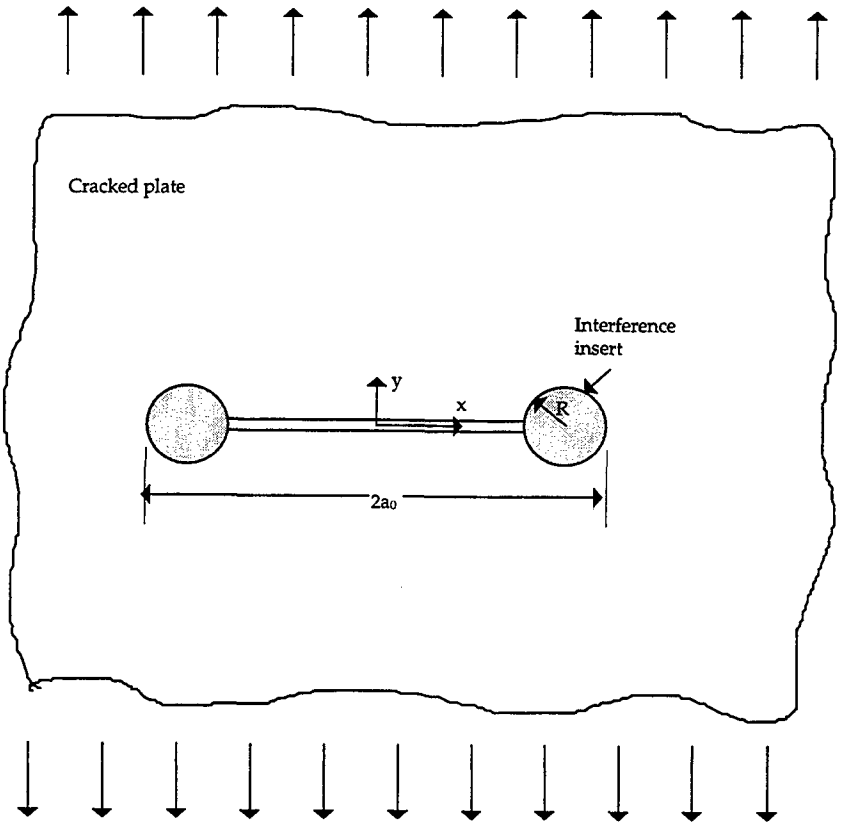

Figure 1. Stop-drilled crack with an interference insert

In this analysis short cracks of *0.066* to *1.0mm* will be considered in the area in which fatigue cracks are expected to re-initiate. It is well known that when the area of plasticity associated with a growing crack is large in comparison to the cracklength, linear elastic fracture mechanics (LEFM) is no longer valid. Hence a more accurate analysis of short cracks can be achieved through the use of an elastic-plastic analysis.

2. Analysis

The F.E. analysis has been carried out using ABAQUS/Standard. This program has the required contact analysis, non-linear geometry and plastic stress analysis capability. The material is a 2024-T851 alloy and is idealised as a perfectly elastic and perfectly plastic stress state, with material properties as shown in Table I. Currently for plasticity, no closed form solutions exist for the interference bolt in a hole containing a crack. However closed form solutions do exist for the case of the expansion of a mandrel in the hole of an infinite plate, which does not contain a crack.

Table I Material properties for 2025-T851.

Young's modulus (MPa)	Poisson's ratio	Yield stress (MPa)	Thickness (mm)
72188.	.33	435.	3.6

The following closed form solutions will be used for the validation of the analysis.

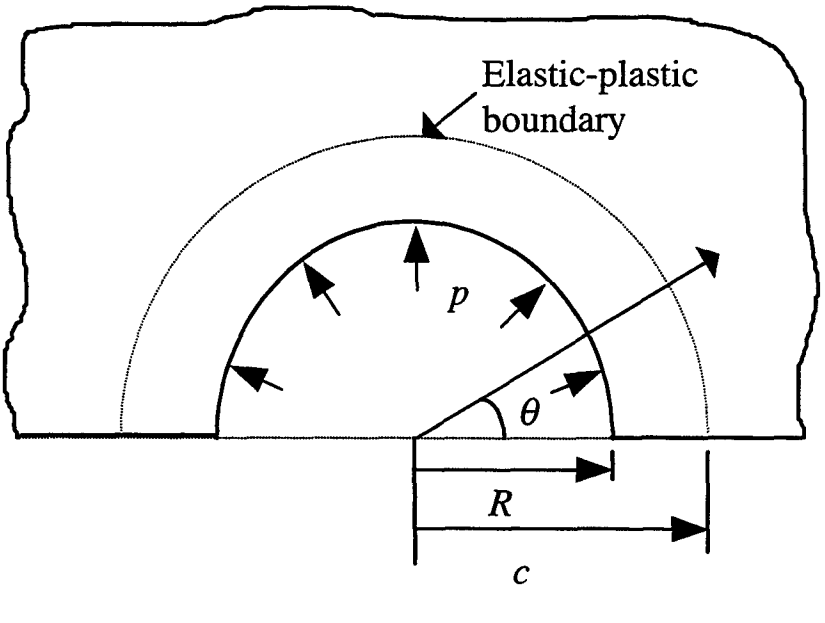

Figure 2. Definition of parameters for analytical expression.

2.1 Step 1: cold-expansion of stop-hole

For the case of hole in an infinite plate (see Figure 2), the stress distribution in the plate and the plug can be determined analytically (Timoshenko and Goodier, 1970). Assuming that the plate material obeys an elastic-perfectly plastic stress-strain relationship, the stresses in the plate after cold-expansion by a mandrel are given by (Jost, 1988),

$$\frac{\sigma_r}{\sigma_0}=\frac{1}{\sqrt{3}}\left[2\ln\frac{r}{c}-1\right],\ \frac{\sigma_\theta}{\sigma_0}=\frac{1}{\sqrt{3}}\left[2\ln\frac{r}{c}+1\right],\ \frac{\sigma_z}{\sigma_0}=\frac{1}{\sqrt{3}}2\ln\frac{r}{c} \tag{1}$$

in the plastic region surrounding the hole and

$$\frac{\sigma_r}{\sigma_0}=-\frac{1}{\sqrt{3}}\left(\frac{c}{r}\right)^2,\ \frac{\sigma_\theta}{\sigma_0}=\frac{1}{\sqrt{3}}\left(\frac{c}{r}\right)^2,\ \sigma_z=0 \tag{2}$$

in the elastic region. Here c denotes the boundary between plastic region and elastic region, which can be determined from the following equation,

$$\lambda\frac{E}{\sigma_0}=\frac{1}{\sqrt{3}}\left\{(1+\nu)\left[\frac{c}{R}\right]^2+(1+\nu_m)(1-2\nu_m)\frac{E}{E_m}\left[2\ln\frac{c}{R}+1-\frac{c^2}{R^2}\right]\right\} \tag{3}$$

where E, ν, σ_0 are respectively the Young's modulus, Poisson's ratio, yield stress of the plate material, and E_m and ν_m are the Young's modulus and Poisson's ratio of the mandrel.

2.2 Step 2: removal of expansion mandrel

Upon the removal of the mandrel, recovery can either be elastic or elastic-plastic depending whether or not re-yielding occurs. The condition for re-yielding is

$$\frac{c}{R}\geq\sqrt{e}\approx 1.65 \tag{4}$$

When the recovery is entirely elastic, the stress distributions are

$$\frac{\sigma_r}{\sigma_0}=\frac{1}{\sqrt{3}}\left\{\left[2\ln\frac{r}{c}-1\right]+\left[2\ln\frac{c}{R}+1\right]\left(\frac{R}{r}\right)^2\right\} \tag{5}$$

$$\frac{\sigma_\theta}{\sigma_0}=\frac{1}{\sqrt{3}}\left\{\left[2\ln\frac{r}{c}+1\right]-\left[2\ln\frac{c}{R}+1\right]\left(\frac{R}{r}\right)^2\right\} \tag{6}$$

for $R<r<c$ and

$$\frac{\sigma_r}{\sigma_0}=-\frac{1}{\sqrt{3}}\left\{\left(\frac{c}{r}\right)^2-\left[2\ln\frac{c}{R}+1\right]\left(\frac{R}{r}\right)^2\right\} \tag{7}$$

$$\frac{\sigma_\theta}{\sigma_0}=\frac{1}{\sqrt{3}}\left\{\left(\frac{c}{r}\right)^2-\left[2\ln\frac{c}{R}+1\right]\left(\frac{R}{r}\right)^2\right\} \tag{8}$$

for $r>c$.

When re-yielding occurs, the radius (ρ) of the re-yield region is given by

$$\rho = \sqrt{\frac{Rc}{\sqrt{e}}} \tag{9}$$

and the stresses in the re-yielded zone are:

For the zone $R \le r < \rho$:

$$\frac{\sigma_r}{\sigma_0} = -\frac{2}{\sqrt{3}}\ln\frac{R}{r},\ \frac{\sigma_\theta}{\sigma_0} = -\frac{2}{\sqrt{3}}\left[1+\ln\frac{R}{r}\right],\ \frac{\sigma_z}{\sigma_0} = -\frac{1}{\sqrt{3}}\left[1+2\ln\frac{R}{r}\right] \tag{10}$$

For the zone $\rho \le r < c$:

$$\frac{\sigma_r}{\sigma_0} = \frac{1}{\sqrt{3}}\left\{\left[2\ln\frac{r}{c}-1\right]+2\left(\frac{\rho}{r}\right)^2\right\},\ \frac{\sigma_\theta}{\sigma_0} = \frac{1}{\sqrt{3}}\left\{\left[2\ln\frac{r}{c}+1\right]-2\left(\frac{\rho}{r}\right)^2\right\} \tag{11}$$

$$\frac{\sigma_z}{\sigma_0} = \frac{1}{\sqrt{3}}\left[2\ln\frac{r}{c}\right] \tag{12}$$

For the zone $r \ge c$:

$$\frac{\sigma_r}{\sigma_0} = \frac{1}{\sqrt{3}}\left\{-\left(\frac{c}{r}\right)^2+2\left(\frac{\rho}{r}\right)^2\right\},\ \frac{\sigma_\theta}{\sigma_0} = \frac{1}{\sqrt{3}}\left\{\left(\frac{c}{r}\right)^2-2\left(\frac{\rho}{r}\right)^2\right\} \tag{13}$$

2.3 Step 3: insertion of interference plug

For small interference, the deformation around the hole should remain elastic, especially when the material around the hole is already under compression as a result of cold-expansion.

The interference pressure is given by,

$$p = \frac{E\lambda}{(1+\nu)+(1+\nu_m)(1-2\nu_m)\dfrac{E}{E_m}} \tag{14}$$

and the corresponding elastic stress distribution is given by

$$\sigma_r = -p\left(\frac{R}{r}\right)^2,\ \sigma_\theta = p\left(\frac{R}{r}\right)^2 \tag{15}$$

The final stress distribution can be readily obtained by superimposing the solutions determined for the above three steps. Comparison with finite element results will be discussed in the next section together with the results corresponding to cold-expanded stop-hole fitted with an interference plug.

3. Finite Element Analysis of Cold-expansion of a Stop-hole

3.1 Step 1: cold-expansion

The stress distributions around a stop-hole determined by an finite element analysis are shown in Figure 3 together with the stress distribution corresponding to a hole in an infinite plate. It can be seen that in the region $\theta < 100^0$, there is a reasonable agreement (with a difference about 10%) between the stress distributions (both tangential and radial stresses) in an infinite plate and a stop-hole, indicating that the influence of the long crack is mainly limited to a region near the intersection between the crack and the hole.

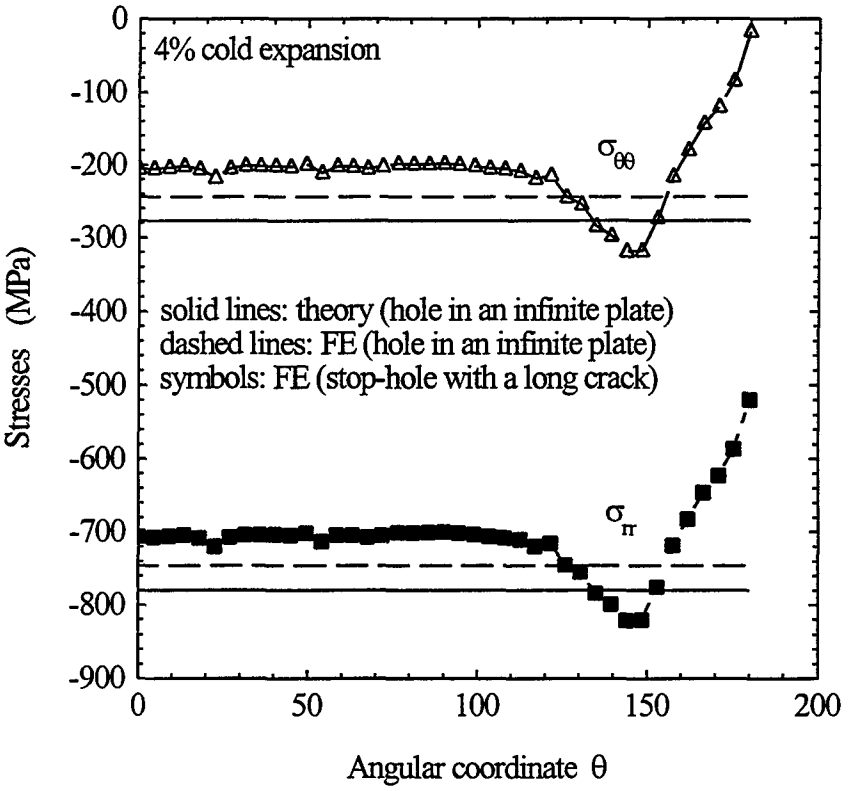

Figure 3. Stress distributions around a cold-expanded hole and stop-hole at 4% expansion.

3.2 Step 2: removal of mandrel

During the removal of the mandrel, further compression yielding occurred in the tangential direction around the hole, as marked by the lower compressive tangential

stress shown in Figure 4 as compared to that shown in Figure 3. Again, in the region $\theta < 100^0$, the stress distribution is nearly unaffected by the presence of the long crack.

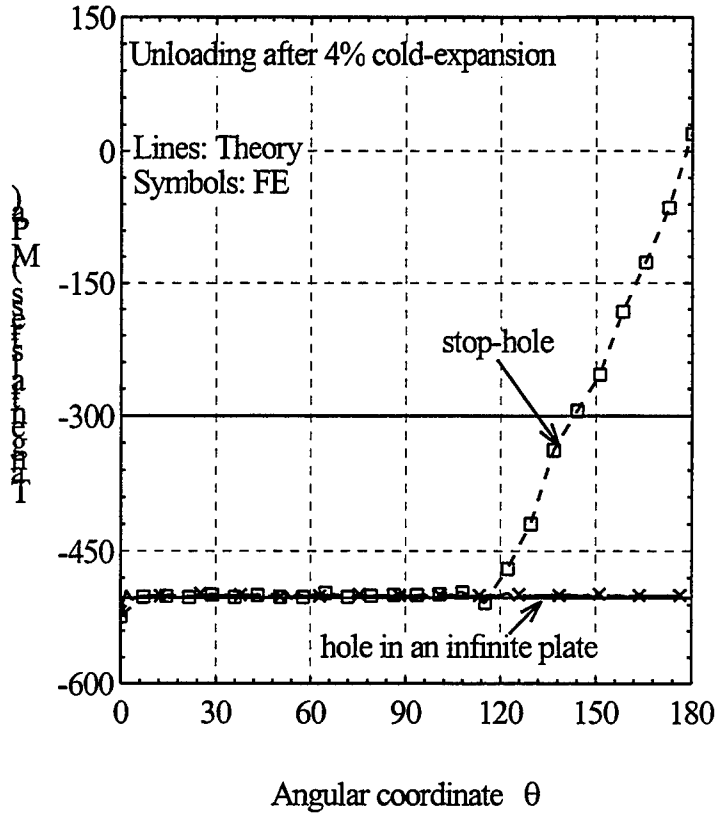

Figure 4. Residual tangential stress after the removal of mandrel.

3.3 Step 3: Insertion of interference plug

Upon insertion of an interference plug into the cold-expanded stop-hole, the residual tangential stress around the hole is reduced in magnitude; the finite element results are shown in Figure 5 together with the results for the analogous problem of a hole in an infinite plate. It is seen that except near $\theta = 0$ for the two cases, there is a considerable difference between the tangential stress distribution around the hole. Consequently the analytical method developed for a hole in an infinite plate is no longer applicable and finite element analysis has to be adopted. The tangential stress distribution away from the hole edge ($\theta = 0$) is shown in Figure 6, indicating a good correlation between the theoretical prediction and the finite element results in the case of a hole in an infinite plate. It is also important to note that as far as the tangential stress distribution away from the hole is concerned, the analytical predictions are still in good agreement with the finite element results.

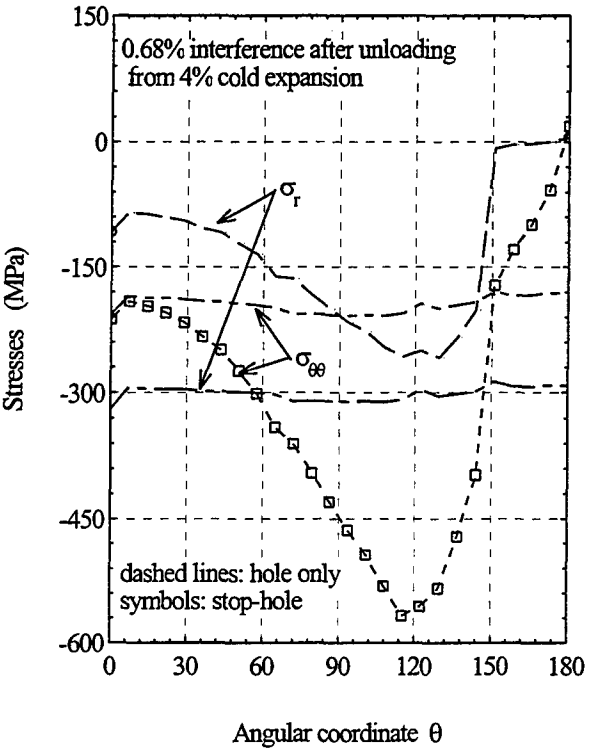

Figure 5. Stress distribution after the insertion of an interference plug ($\lambda = 0.67\%$).

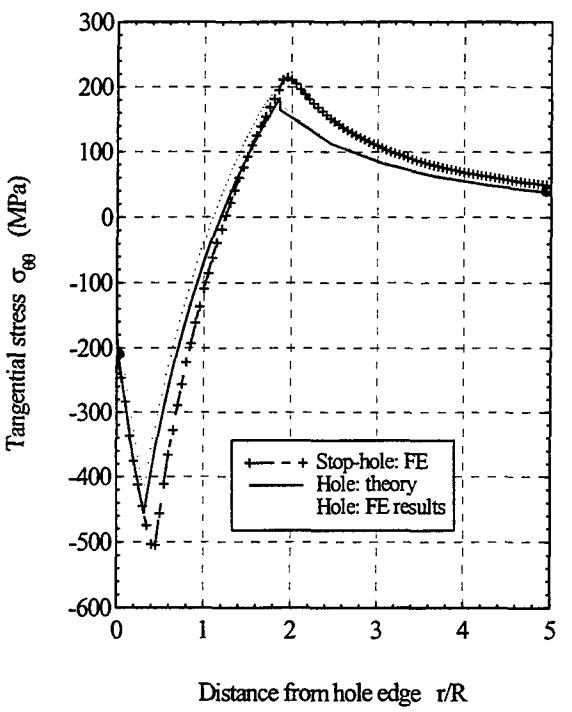

Figure 6. Distribution of the tangential stress around of a cold-expanded hole in an infinite plate followed by insertion of a interference plug ($\lambda = 0.67\%$).

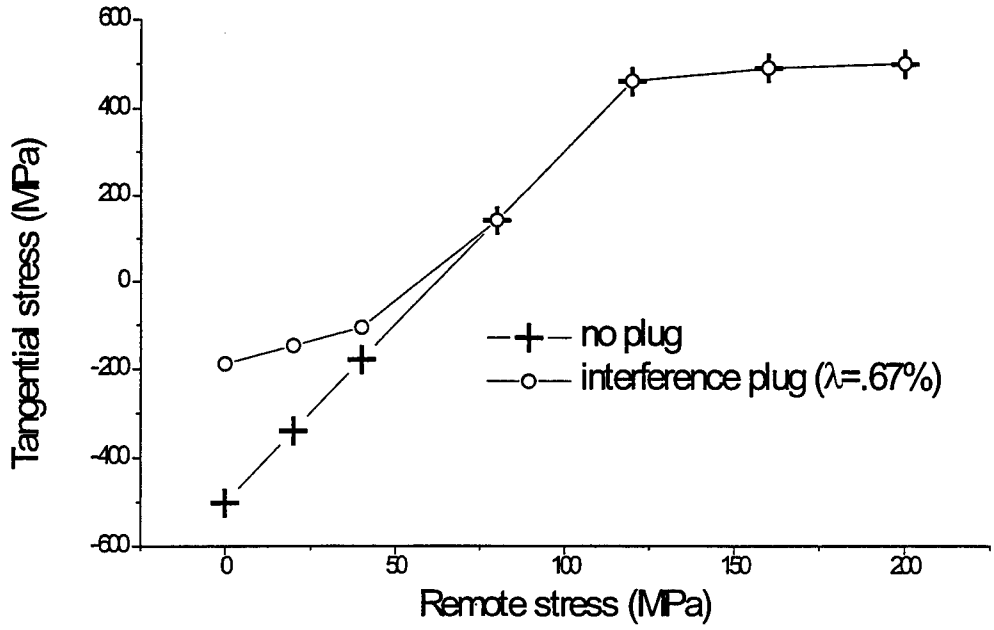

Figure 7. Tangential stress at edge of cold expanded hole versus remote stress for case of no plug and interference plug.

4. Application of Remote Load to Combined Interference Fitting and Cold-Expansion of Stop-holes

To examine the overall benefit of combined interference fitting and cold-expansion of the stop-hole in improving fatigue life of cracked structures, remote tension is applied to the complete geometry. The tangential stresses ahead of the hole crack at different applied load levels are shown in Figure 7. For comparison purposes, the tangential stress distribution corresponding to the case of cold-expanded stop-hole without an interference plug is also included in the figure. The Young's modulus assumed for the plug is *210000MPa,* and poisson's ratio *is .3* . One important observation that can be made from the results is shown in Figure 7. The rate of increase in the tangential stress at the hole edge for the case fitted with an interference plug is only slightly lower than the case without interference plug. This implies that under tension dominated loading, the interference plug may not provide any extra benefit than a cold-expanded stop-hole. A comparison of the tangential stress at $\theta=0$ at the edge of the hole versus the remote applied load shown in Figure 8, shows no improvement for the interference fit plug. However, it is expected that when the far field load has compression components, as normally encountered in many aircraft structures, the addition of an interference plug is beneficial in eliminating local reverse yielding near the stop-hole.

This is further illustrated in Figure 9 which shows the deformed geometry corresponding to a remote stress of 200 MPa. Clearly, due to the presence of the long crack, the stop-hole opens up and the plug is totally detached from the hole. The contact modelling procedure involves a master-slave concept in which the mandrel corresponds to the master and the aluminium plate the slave. The solution is iterative in that the initial contact surface must be assumed and an improvement on this assumption is obtained after each solution, until convergence is achieved. The change in geometry may require a large displacement analysis to be carried out. In the next section the advantages of interference will be considered under remote cycling loads.

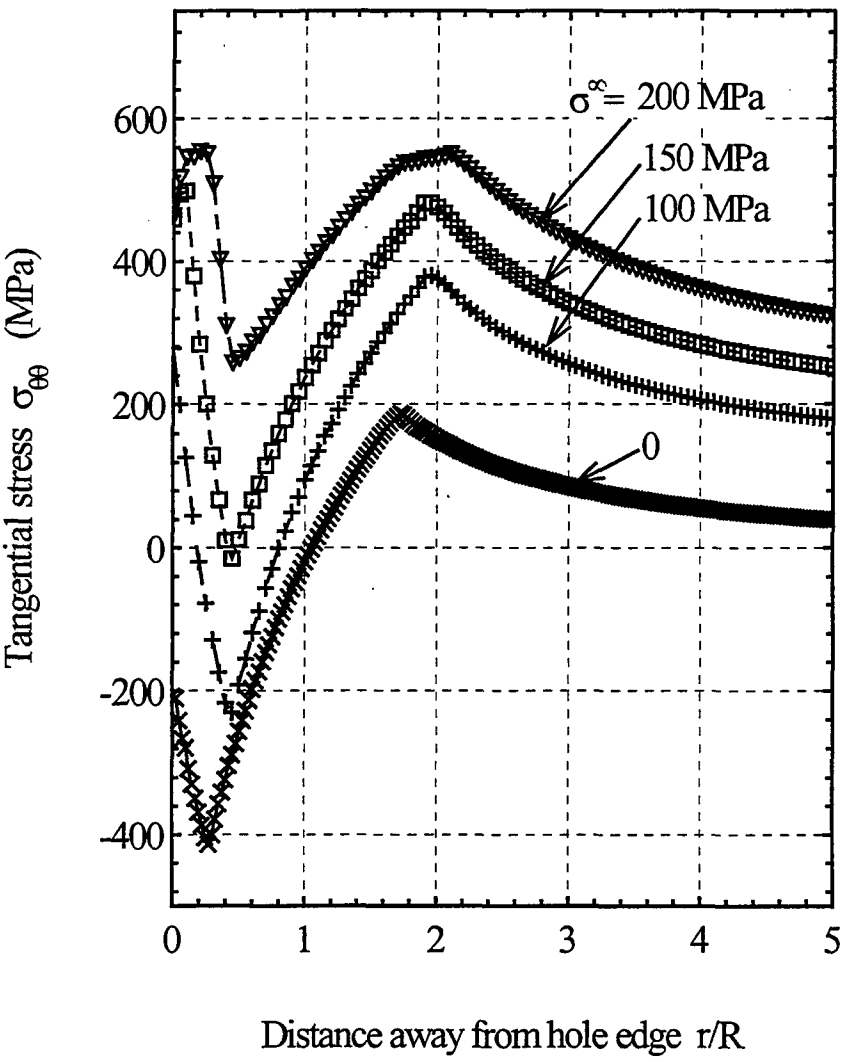

Figure 8. Tangential stress distribution ahead a cold-expanded hole fitted with an interference plug subjected to remote load.

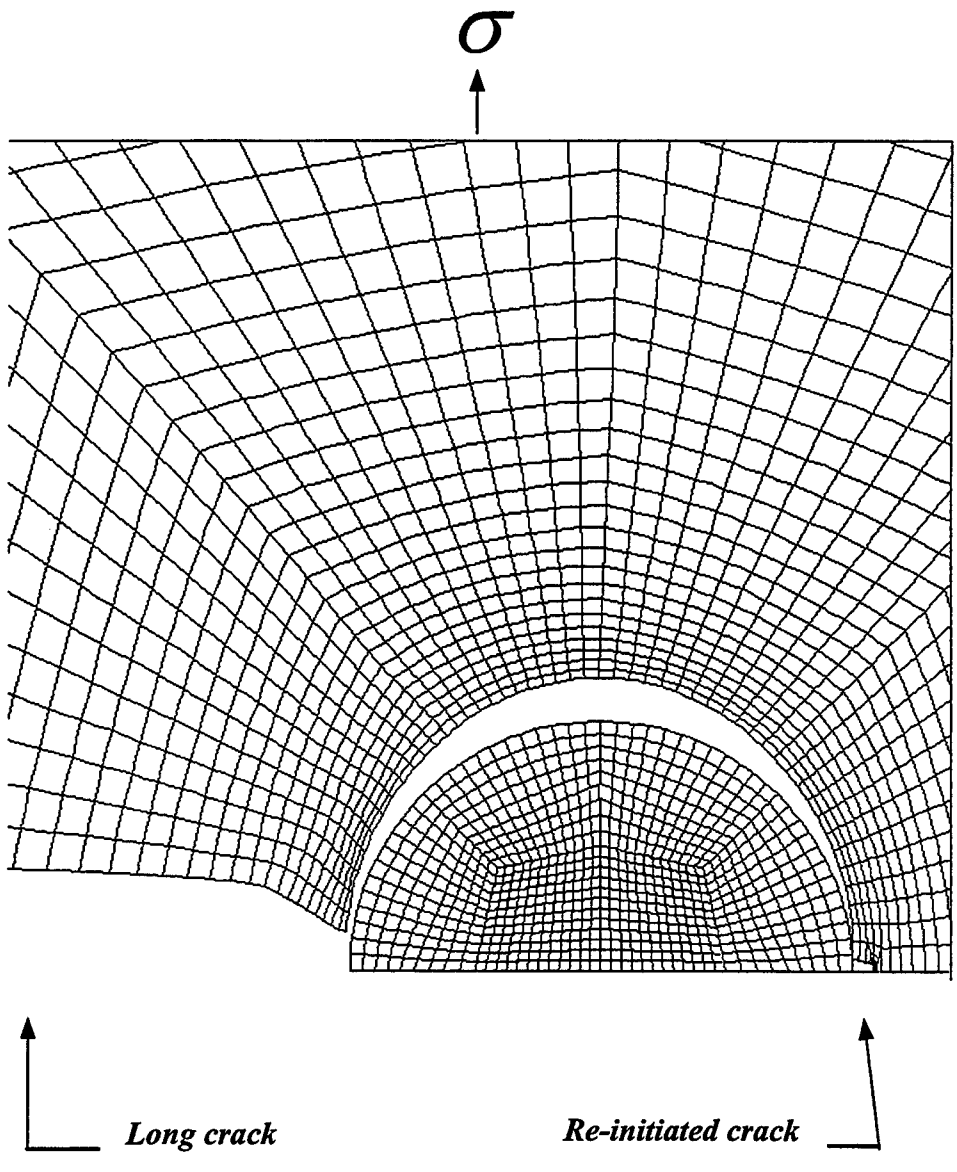

Figure 9. F.E. mesh, ¼ symmetry, deformed plot corresponding to remote stress of 200MPa, shows that the interference plug has no influence for maximum tensile loads.

5. Stress Analysis: Interference Plug Subject to Cyclic Load

5.1 Tangential stress and load level

In order to understand the fatigue behaviour of a short crack an analysis has been carried out for the first 5 cycles where the applied stress ranges from 0-200MPa. For

this configuration only a long crack exists, with prior expansion of the hole. The stress to be considered is the tangential stress located at the point at which a short crack would seem most likely to initiate. Two cases are considered, the first corresponds to the case in which a plug is not used during loading, while the second case involves the use of an interference plug. In Figure 10 a plot of tangential stress versus applied stress is shown for the case of no plug. For this case the stress cycle starts at an applied remote stress of zero, as shown by the arrow. The tangential stress at this point is -500MPa due to cold expansion. Note that the stress at which yielding occurs for plane strain is $\sigma_0.2/\sqrt{3} = 500.MPa$. Increasing the applied load stress to 100MPa results in a linear variation of tangential stress to a maximum value of 500MPa at which yielding occurs. Increasing the applied stress to 200MPa maintains the tangential stress at 500MPa. Unloading, as shown by the arrow, to an applied stress of 80MPa results in a linear variation of tangential stress to approximately -500MPa. Unloading to zero maintains the tangential stress at approximately -500.MPa. Subsequent cycles follow this identical path.

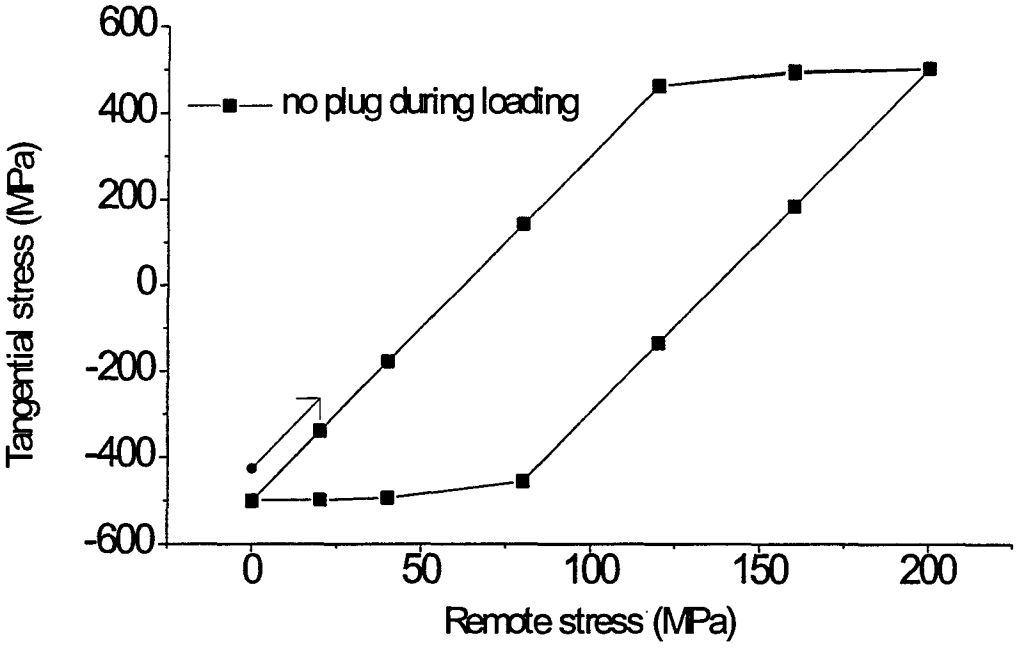

Figure 10. Variation of tangential stress with applied stress for case in which no plug is used during loading.

At this point it is useful to make a comparison with the case in which an interference plug is present during loading. The results for this case are shown in Figure 11, where the arrows show the load cycle. In comparison to Figure 10 significant differences exist. Firstly, the presence of an interference plug results in an initial stress of -200MPa at zero load, in comparison with -500MPa shown in Figure 12. In Figure 11 the initial

loading to 160MPa shows a non-linear response, which is due to the influence of the plug. Further loading to 200MPa results in a tangential stress of 500MPa. The unloading curve is similar to that in Figure 10, except that a maximum compressive stress of -550MPa occurs. The reason for this is that under compression the plug does not allow the hole to deform and relieve the radial contact pressure at that point, which due to poissons ratio increases the tangential stress. Note that as shown by the arrows, the second cycle does not follow the first cycle, however all subsequent cycles are identical. In comparison to the no plug case, the most significant differences occur with the gradients of the compressive loading/unloading curves.

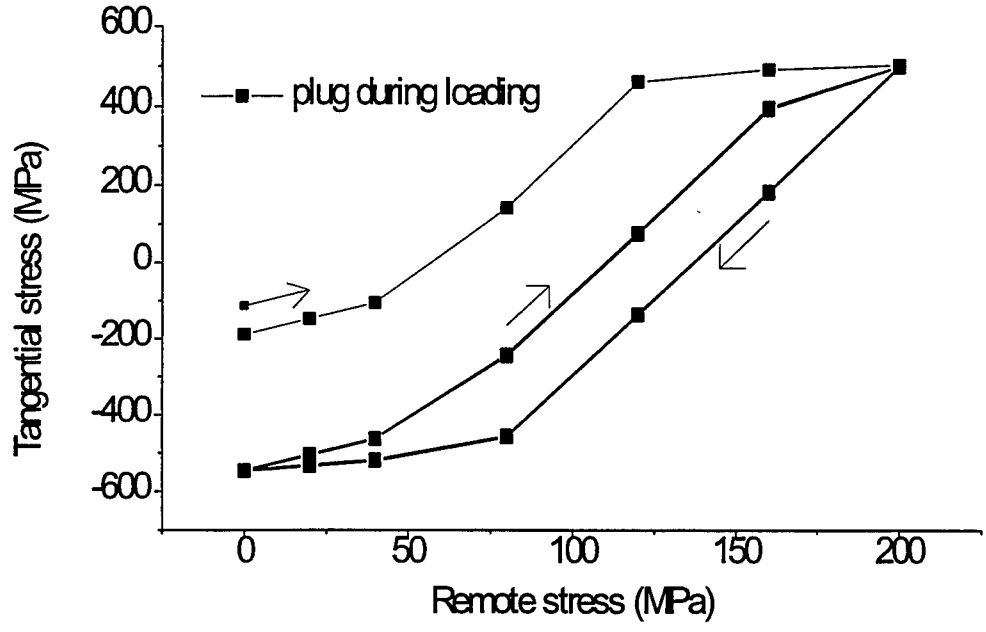

Figure 11. Variation of tangential stress with applied stress for case of interference plug used during loading.

5.2 Stress/strain curves

The location of interest is still at the region at which otherwise a small crack would initiate. For this location the stress/strain plot corresponding to the no plug case is shown in Figure 12. Again, the arrows show the initial loading and cyclic behaviour. These curves exhibit the perfectively elastic perfectively plastic behaviour during loading and unloading. Clearly for tangential stresses greater than 500MPa yielding is occurring and strains change significantly. Note that all cycles show an identical path.

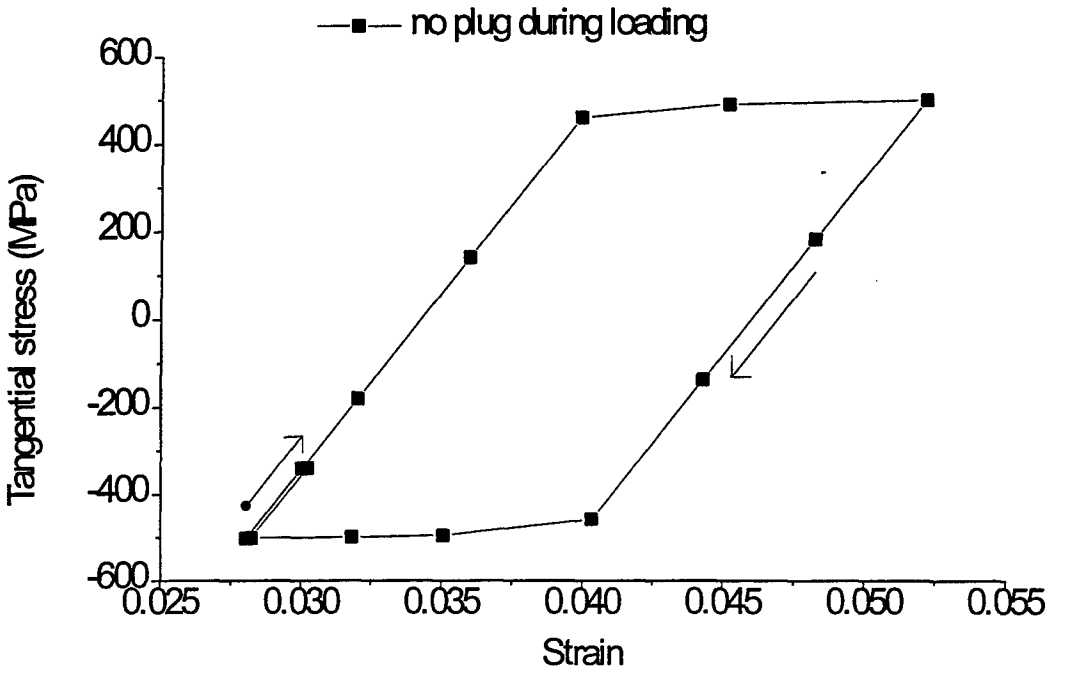

Figure 12. Stress/strain plot for case of no plug during loading.

For the case of an interference plug used during loading, the results are shown in Figure 13, where the arrows show the initial loading corresponding to the lowest value of strain, and the subsequent load path. The lowest value for strain occurs at a compressive stress of -200MPa which corresponds to the fitting of an interference plug. For the first cycle after the yield stress has been reached a considerable strain occurs during loading. However all subsequent cycles result in a considerably reduced range of strain values in comparison to the first cycle. The hysteretic plastic work per cycle can be regarded as a correlating parameter for fatigue damage accumulation. The comparison of stress/strain curves for the no plug case and interference plug are shown in Figure 14. Except for the first cycle, it is evident that the hysteretic plastic work for the no plug case is approximately double the case in which the interference fit plug is used. As a result the expected fatigue life for the case in which a plug is used would be expected to be significantly greater. Note also that with the use of an interference plug a slight increase in stress amplitude occurs.

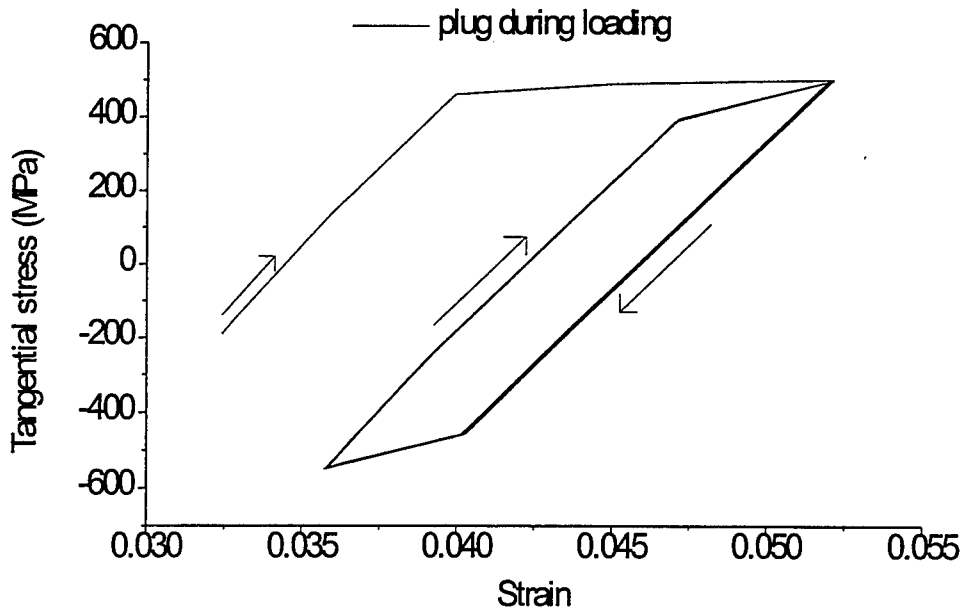

Figure 13. Stress/strain plot for case of use of interference plug during cyclic loading.

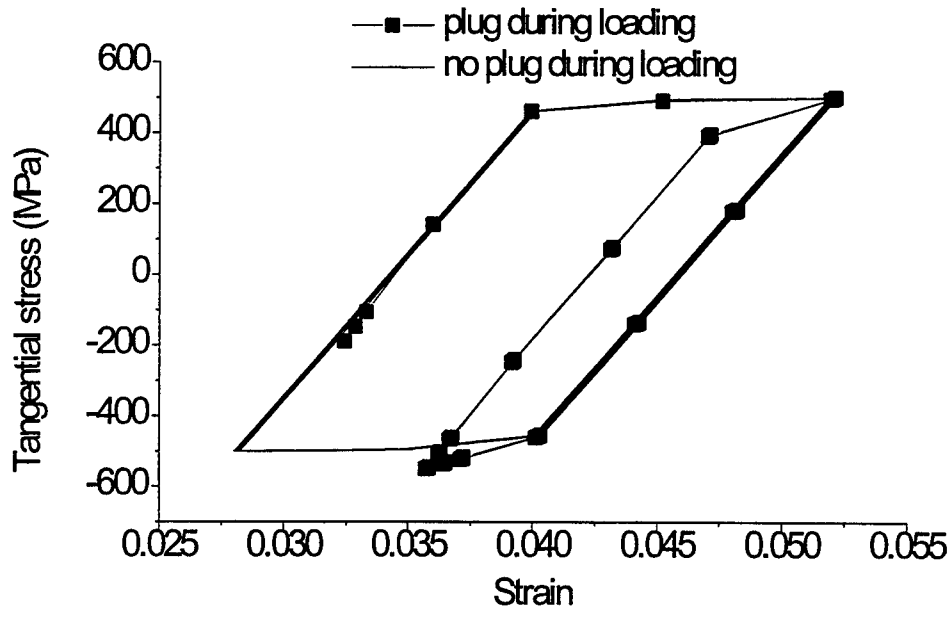

Figure 14. Stress/strain comparison plots for case of plug during loading and case of no plug during loading.

6. Computation of Stress Intensity Factor of Re-initiated Crack

6.1 Analytical approach

When the enhanced specimens are subjected to remote loading, depending upon the level of the applied load, plastic deformation may occur ahead of the stop-hole, leading to new crack growth, as depicted in Figure 15. Here we will first examine the growth behaviour of a re-initiated crack; the issue of crack initiation will be addressed later.

The prospective stress distributions along a newly initiated crack at various applied stress levels are shown in Figure 8. For a small crack of length a_1 re-initiated at the tip of the stop-hole, the stress intensity factor can be computed using a Green function (Grandt, 1975; Ball,1990)

$$K = \int_0^{a_1} G(r, a_1)\sigma_{\theta\theta}(r)dr \qquad (16)$$

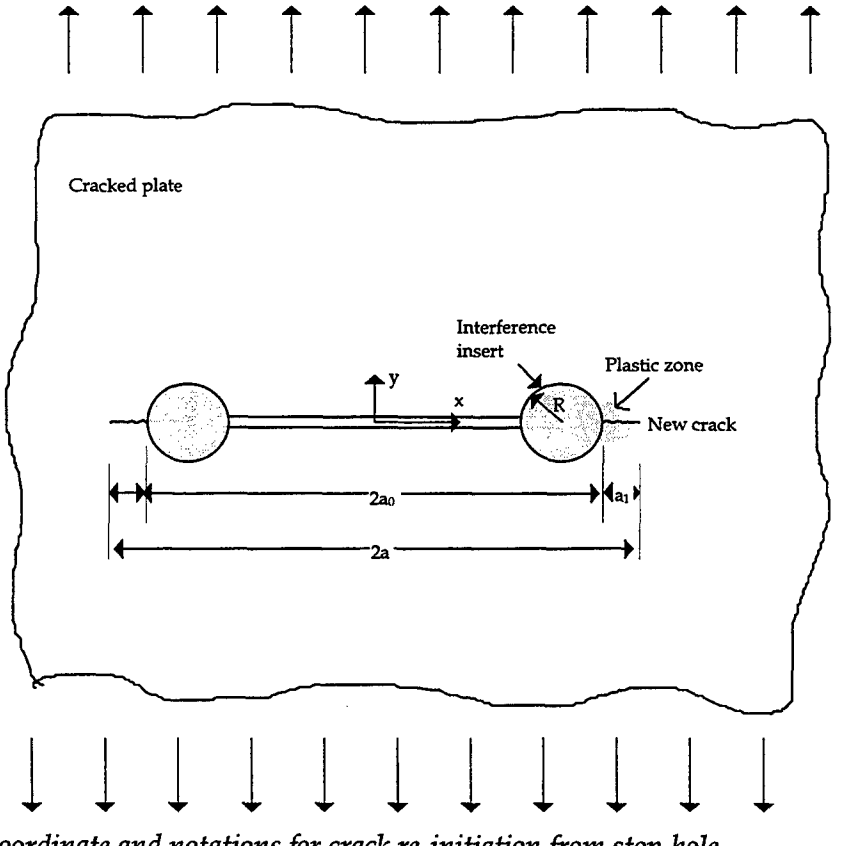

Figure 15. Coordinate and notations for crack re-initiation from stop-hole

where the function $G(r,a_1)$ denotes the stress intensity factor of a crack a_1 caused by a point force acting at position r. The exact Green function does not appear to exist for a short crack emanating from a stop-hole. In the following we will make use of the limiting solutions for $a_1 << R$ and $a_1 >> R$ to provide lower and upper bound solutions.

For $a_1 << R$, the problem can be treated as an edge crack in an infinite plate (Tada,1974),

$$G_s(r,a_1) = \frac{2}{\sqrt{\pi a_1}} \frac{1.3 - 0.3(r/a_1)^{3/2}}{\sqrt{1-(r/a_1)^2}} \tag{17}$$

and for $a_1 >> R$, the Green function is that for a point force acting on a line crack in an infinite plate, which is well known,

$$G_l(r,a_1) = \frac{1}{\sqrt{\pi(a+a_1)}} \sqrt{\frac{2a_0 + a_1 + r}{a_1 - r}} \tag{18}$$

Here the subscripts s and l are used to denote the Green functions pertaining to the short crack bound and the long crack bound. As seen in Figures 16 and 17 , these two solutions provide reasonable bounds to the stress intensity factor.

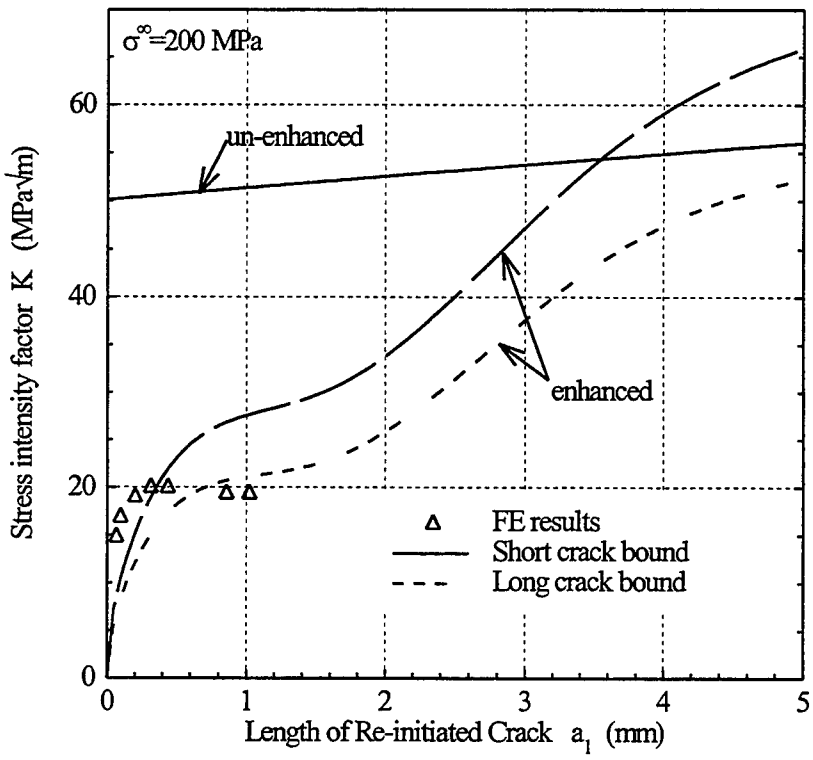

Figure 16. Stress intensity factor versus crack length for remote stress equal to 200 MPa.

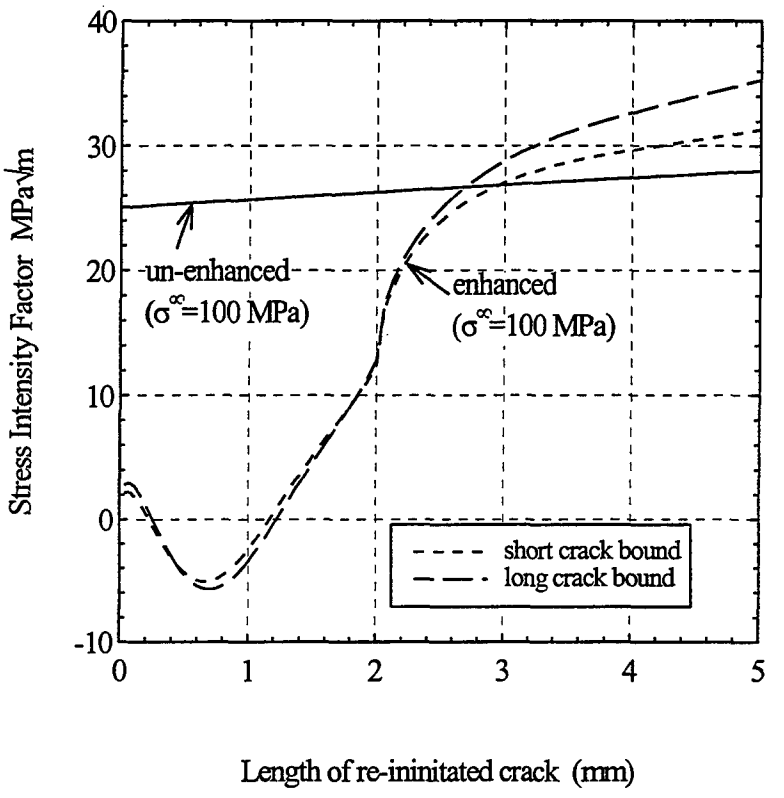

Figure 17. Stress intensity versus crack length for short and long crack bounds.

6.2 Method for computation of stress intensity factors

The following is a brief account of the basis on which the plastic stress intensities are computed, for a monotonic loading. A more detailed account is given in the Appendix. The method outlined here is not applicable to cycling loading. For fully plastic solutions, (Goldman and Hutchinson, 1975) give the displacement field at the crack tip for mode I opening as:

$$u_y = \alpha.\varepsilon_0 K_\varepsilon r^{1/(n+1)} \tilde{u}_y(\theta) \qquad \ldots(19)$$

where α is a material constant
ε_0 is a reference value of strain (yield)
n is the work hardening exponent

where K_ε is the plastic strain intensity factor

Finite Element solutions have been considered (Shih, 1981) for the case of small scale yielding. An evaluation of the crack tip opening displacement (CTOD) is

defined at a point in which a 45^0 line intersects the crack profile shown in Figure 18. The equation is:

$$r - u_x = \frac{\delta_t}{2} \qquad \ldots(20)$$

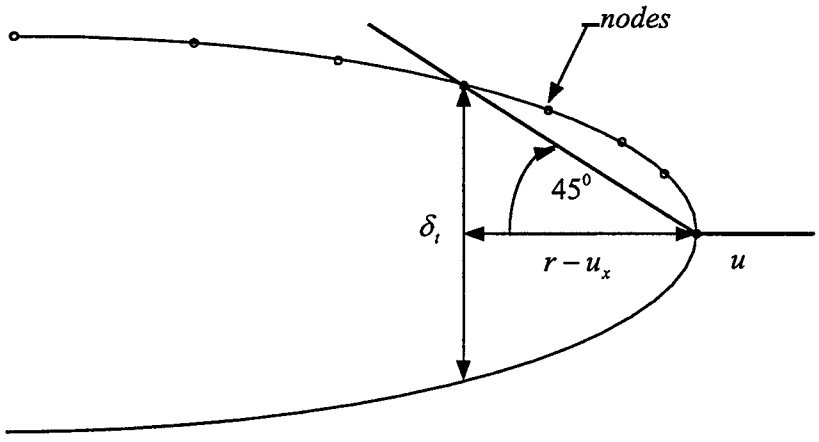

Figure 18. Intersection of 45^0 line and the crack profile.

The value of δ that satisfies equ(20) is given by:

$$\delta_t = d_n \frac{J}{\sigma_0} = CTOD \qquad \ldots(21)$$

Since $J = K^2 / E$ we have:

$$K = \sqrt{\frac{E\sigma_0 CTOD}{d_n}} \qquad \ldots(22)$$

where σ_0 is the yield stress.

6.3 Discussion on analytical and F.E. analysis

It has been found that to compute the plastic stress intensity factor using the F.E. method it is necessary to have a fine mesh with crack tip elements of the size of *.0001mm.* In Figure 19 the crack-face displacements are shown at the crack tip for a crack-length of 0.097mm. The intersecting 45^0 line, as discussed in section 6.1 is also shown and gives the CTOD solution from which stress intensities may be computed. Each data point behind the crack tip represents a node in the mesh, and it is evident that in this case values of CTOD are only achieved for load levels of 100MPa and above.

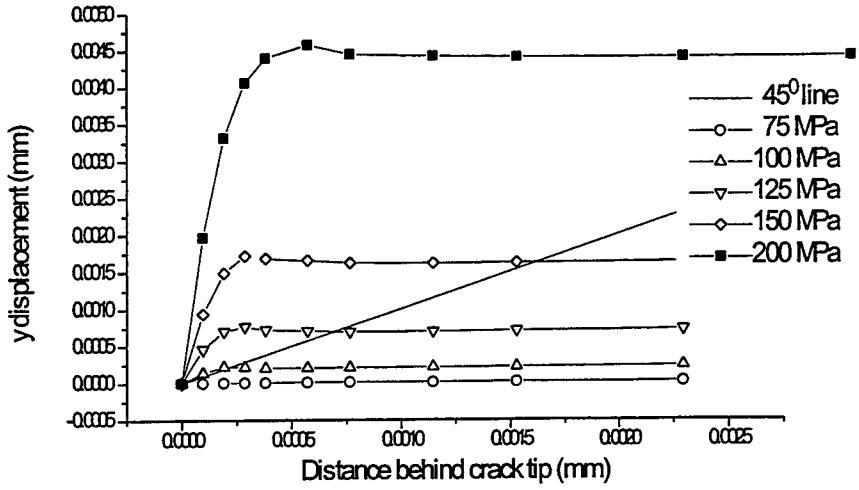

Figure 19. y displacement versus distance behind crack tip, for a range of applied stresses corresponding to a crack-length of 0.0979mm.

As mentioned previously a number of short cracks of crack-lengths of $a = 0.066$ to *1.0mm* have been considered for a remote applied stress of 200MPa and are shown in Figure 20. The corresponding stress intensities are those shown in Figure 16. Results from cycling the applied remote stress are shown in Figure 21, where the arrow corresponding to a zero CTOD defines the initial loading and other arrows show the cyclic loading path. In this case only the CTOD has been considered since the procedure for computing stress intensity factors corresponding to unloading is more complex than the procedure for monotonic loading outlined in section 6.1 . Note that except for the first cycle of loading the cycling follows an identical path.

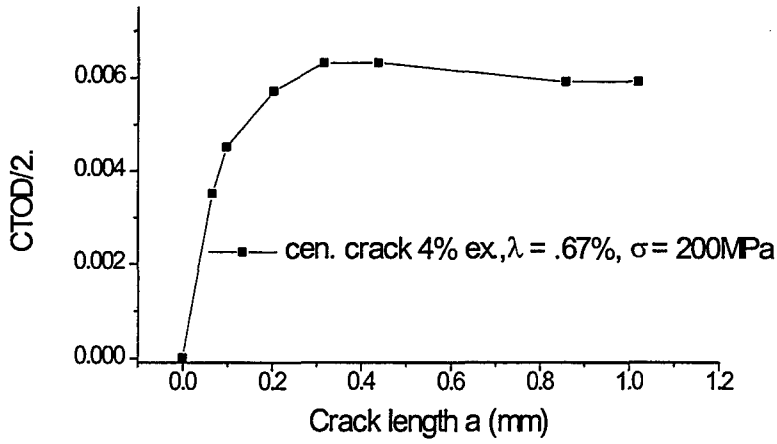

Figure 20. Values of CTOD versus cracklength for a range of cracklengths, enhanced, λ =.67%., remote load = 200MPa

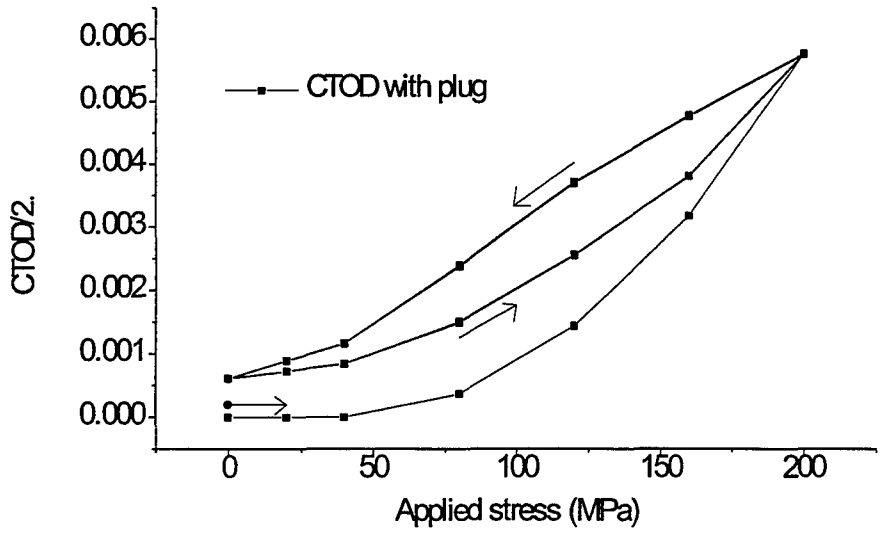

Figure 21. Variation of crack opening displacement with applied stress for 5 cycles, a_1 = 0.0997mm, Stress ratio=0, a_o = 20mm.

It is clear from Figure 17 that for the same applied stress of 100 MPa, the driving force for a re-initiated crack increases initially and then decreases below zero, indicating a crack arrest even when a new crack has been initiated at the hole edge. This means that the enhanced geometry should yield infinite fatigue life for an applied stress equal to

100 MPa. This is primarily caused by the compressive tangential stress between 0.2 and 0.8 times the hole radius.

When the applied stress is increased to 150 MPa, as shown in Figure 8, the tangential stress becomes positive everywhere, and hence any new crack initiated at the hole edge will continue to grow to failure.

When the applied stress is further increased to 200 MPa, some degree of plastic yielding occurs at the edge of the hole. However, when the above results are compared with those determined from finite element, as indicated by symbols in Figure 16, the analytical method considerably underestimates the stress intensity factor. This is most likely due to the fact that the influence of plasticity near the hole was not accounted for in the analytical method. The extent of the plastic deformation was approximately 20% of the stop-hole radius. The results shown in Figure 16 suggest that once the newly initiated crack reaches about 0.3mm, it will grow at much the same rate as the un-enhanced crack.

6.4 Fatigue life prediction

This is further demonstrated in Figure 22, where the experimental data are taken from (Finney *et al*, 1996). It is seen from Figure 22 that FASTRAN II is able to provide a very good prediction of the fatigue crack growth curve for the un-enhanced specimen.

In this case the growth rate is determined from the following equation (used in FASTRAN II):

$$\frac{da}{dN} = C\left(\Delta K_{eff}\right)^m \left[1 - \left(\frac{\Delta K_{th}}{\Delta K_{eff}}\right)^2\right] \qquad (23)$$

where the constants corresponding to 2024-T851 may be determined from the Damage Tolerant Handbook and are given by:

$C = 7.4x10^{-10}$

$\Delta K_{th} = 1.0 MPa\sqrt{m}$

$m = 2.93$

$\alpha = 1.9$ (constraint factor required by FASTRAN II)

In the case of the enhanced specimen, once the crack length exceeds 0.3mm, the prediction is in good agreement with the experimental data. At the moment, it is not clear how we can predict the crack growth behaviour for crack lengths less than 0.3mm, which is the key to determining the total fatigue life of the enhanced structure. For short crack lengths, local plasticity near the hole edge plays a significant role in affecting fatigue crack growth rate. Work is currently in progress to develop a methodology which is capable of dealing with short cracks growing from a notch plastic field.

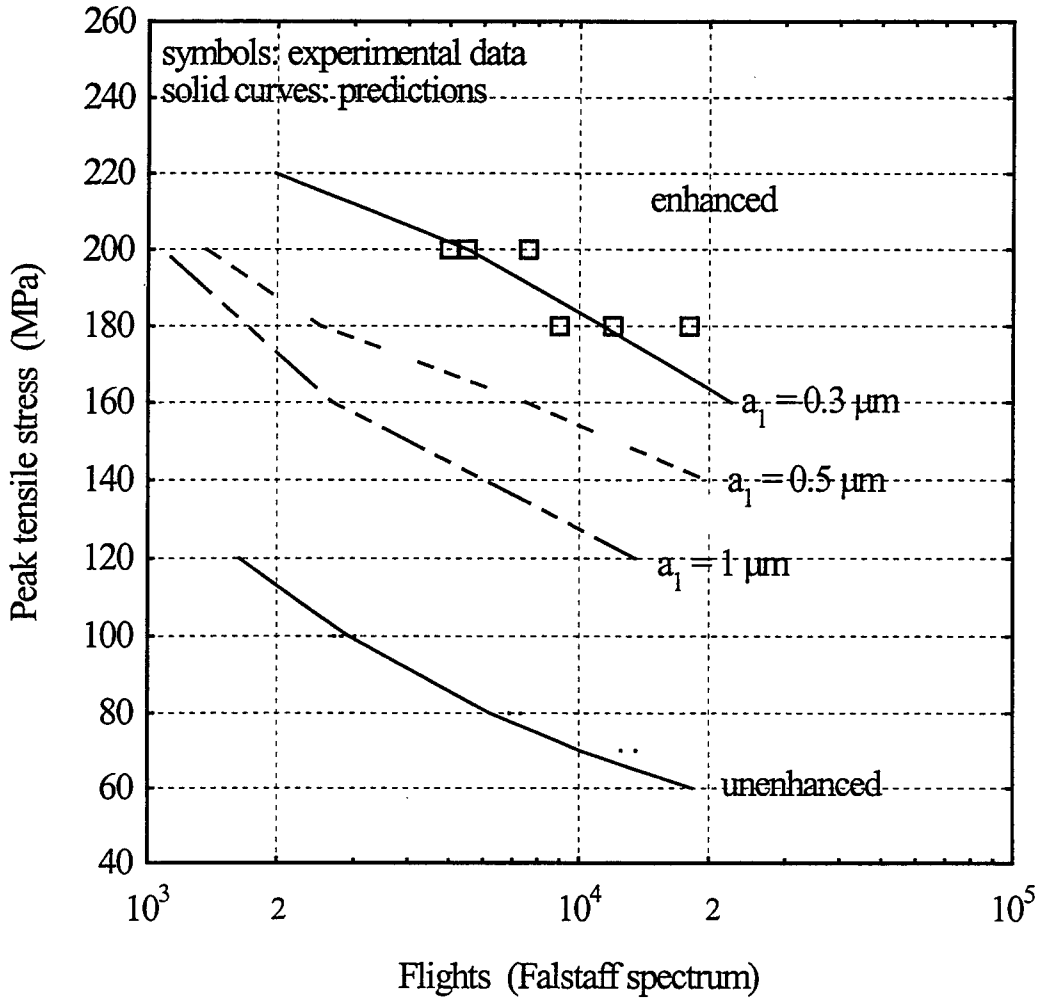

Figure 22. Peak tensile stress versus number of loading blocks for a plain cracked plate and a cracked plate enhanced by a combination of interference fitting and cold-expansion of stop-hole. Symbols: experimental data; solid curves: predictions using FASTRAN II.

7. Conclusions

The following conclusions can be drawn from the present study of a particular improved life enhancement method: combined interference fitting and cold-expansion of stop-hole.

1. In the absence of an applied remote load, the residual stress distribution along the prospective path of a newly initiated crack near a cold-expanded stop-hole (with a long crack) is approximately the same as that which would exist around a cold-expanded hole in an infinite plate.

2. Upon the application of a remote load, the interference of an inserted plug would not only reduce the stress concentration ahead of the stop-hole but also reduce the level of hoop stress at the onset of plastic yielding due to the beneficial effect of the interference pressure on plastic yielding.

3. For the case of cyclic loading it has been found that the combination of interference fitting and cold-expansion of a stop-hole would significantly reduce the magnitude of hysteretic work around the stop hole although some increase in stress amplitude is noticed.

4. After the crack is re-initiated ahead of the stop hole, the value of the crack driving force is found to be considerably greater than the Green's function approach (LEFM).

5. Based on the numerical results of the crack driving force, which accounts for notch plasticity, fatigue life predictions are made using a crack growth code. Provided a suitable initial crack-length is selected, good correlation can be obtained with experimental values.

8. References

Ball, D. (1990) Proposed integration of notch-strain and fatigue crack growth analysis, *J. Aircraft*, Vol.**27**, 358-367.

Domazet, Z. (1996) Comparison of fatigue crack retardation methods, *Engineering Failure Analysis*, Vol.**3**, No.2, 137-147.

Finnery, J. M., Niessen, C., Absolom, N. And Lemm, K. (1996) Strength and fatigue life enhancements of cracked metal, *Technical Report DSTO-TR-0434*.

Grandt Jr., A. F. (1975) Stress intensity factors for some through-cracked fastener holes, *Int. J. Fracture*, Vol.**11**, No.2, 283-294.

Jost, G.S. (1988) Stresses and strains in a cold-worked annulus, *Aircraft Structure Report 434*, Commonwealth of Australia.

Newman, J. C. (1992) FASTRANII-a fatigue crack growth structural analysis program, *NASA Technical Memorandum*, 104159.

Tada, H., Paris, P. C. And Irwin, G. R. (1974) *The Stress Analysis of Cracks Handbook*, 2nd Edition, Del Research Corp., Hellertwon, PA, USA.

Timoshenko, S. P. And Goodier, J. N. (1970) *Theory of Elasticity*, McGraw-Hill International.

Goldman, N.L. and Hutchinson, J.W. Fully Plastic Crack Problems: The Centre - Cracked Strip under Plane Strain. Int. J. Solids Structures, vol. 11. p575-591, 1975.

Hutchinson, J.W. Singular Behaviour at the end of a Tensile Crack in a Hardening Material. J. Mech. Phys. Solids, vol. 16, p13-31, 1968.

Rice, J.R. and Rosengren, G.F. Plane Strain deformation near a crack tip in a Power-Law Hardening Material. J.Mech.Phys.Solids, vol. 16, p1-12, 1968.

Tracey, D.M. Finite Element Solutions for Crack - Tip Behaviour in Small - Scale Yielding. Trans. A.S.M.E. vol. 98, p146-151, April 1976.

Shih, C.F. Relationships between the J - Integral and Crack Opening Displacement for Stationary and Extending Cracks. J. Mech. Phys. Solids. Vol. 29, no.4. p305-326, 1981.

Vulic, N. , Jecic, S. and Grubisic, V. Validation of crack arrest technique by numerical modelling. Int. J. Fatigue Vol. 19, No. 4, p 283-291, 1997.

Anon. Damage Tolerant Design Handbook. A Compoilation of Fracture and Crack-Growth Data for High-Strength Alloys. Vol. 3 , Dec. 1983.

Appendix: Method for Computation of Stress Intensity Factors

The following analysis is the basis on which the plastic stress intensities are computed, as shown in Figure 16, for a monotonic loading. They are not, however applicable to cycling loading.

Fully plastic solutions are considered, (Goldman and Hutchinson, 1975), and the relationship between stress and strain is given in the following form:

$$\frac{\varepsilon}{\varepsilon_o} = \alpha\left(\frac{\sigma}{\sigma_o}\right)^n \qquad \ldots(1)$$

where α is a material constant
ε_0 is a reference value of strain (yield)
σ_0 is a reference value of stress (yield)
n is the work hardening exponent

For fully plastic solutions, (Goldman and Hutchinson, 1975) give the displacement field at the crack tip for mode I opening as:

$$u_y = \alpha.\varepsilon_0 K_\varepsilon r^{1/(n+1)} \tilde{u}_y(\theta) \qquad \ldots(2)$$

where K_ε is the plastic strain intensity factor

This solution is the same as that proposed by (Hutchinson, 1968) and (Rice and Rosengren, 1968) (HRR) for the case of small scale yielding. The HRR near tip behaviour is expressed as:

$$\sigma_{ij} \to r^{-n/(n+1)} \tilde{\sigma}_{ij}(\theta, n) \qquad \ldots(3)$$

$$\varepsilon_{ij} \to r^{-1/(n+1)} \tilde{\varepsilon}_{ij}(\theta, n) \qquad \ldots(4)$$

In order to relate crack opening displacement to J (Tracey, 1976) has expressed the HHR singularity as:

$$\sigma_{ij} = \sigma_0\left(\frac{EJ}{\alpha.\sigma_0^2 I_n r}\right)^{1/(n+1)} \tilde{\sigma}_{ij}(\theta, n) \qquad \ldots(5)$$

$$\varepsilon_{ij} = \frac{\alpha.\sigma_0}{E}\left(\frac{EJ}{\alpha.\sigma_0^2 I_n r}\right)^{n/(n+1)} \tilde{\varepsilon}_{ij}(\theta,n) \qquad \ldots(6)$$

where E is Young's modulus
σ_0 is the yield stress
J is the J Integral

Finite Element solutions have been considered (Shih, 1981) for the case of small scale yielding. An evaluation of the crack tip opening displacement (CTOD) is defined at a point in which a 45^0 line intersects the crack profile shown in Figure A1. The equation is:

$$r - u_x = \frac{\delta_t}{2} \qquad \ldots(7)$$

The choice of a 45^0 angle does have the advantage of restricting the CTOD to near tip values. The terms that satisfy equs(7) are given (Tracey, 1976) as:

$$\delta_t / 2 = \frac{\alpha.\sigma_0}{E}\left(\frac{EJ}{\alpha.\sigma_0^2 I_n}\right)^{n/(n+1)} \frac{1}{r^{n+1}} \tilde{u}_y(n) \qquad \ldots(8)$$

$$u_x = \frac{\alpha.\sigma_0}{E}\left(\frac{EJ}{\alpha.\sigma_0^2 I_n}\right)^{n/(n+1)} \frac{1}{r^{n+1}} \tilde{u}_y(n) \qquad \ldots(9)$$

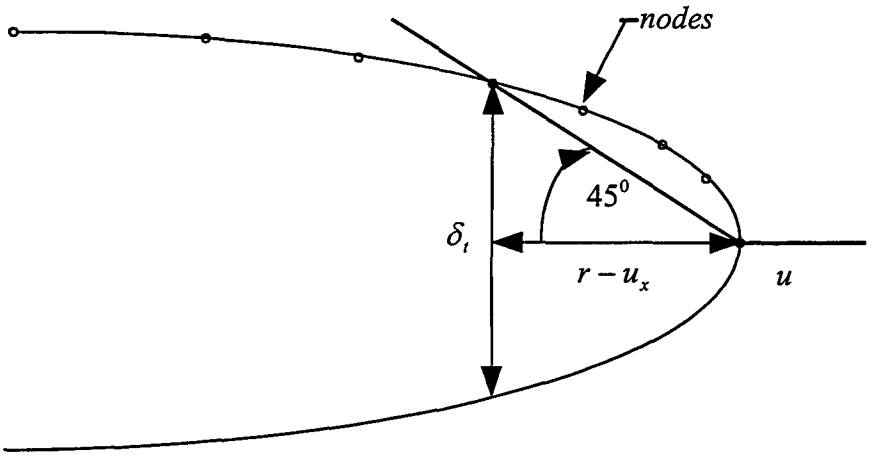

Figure A1. Intersection of 45^0 line and the crack profile.

The value of δ that satisfies equs(7), (8) and (9) is given by:

$$\delta_t = d_n \frac{J}{\sigma_0} = CTOD \qquad \ldots(10)$$

Since $J = K^2 / E$ we have:

$$K = \sqrt{\frac{E\sigma_0 CTOD}{d_n}} \qquad \ldots(11)$$

we also have from (Tracey, 1976):

$$d_n = \left(\frac{\alpha.\sigma_0}{E}\right)^{1/n} \left(\tilde{u}_x + \tilde{u}_y\right)^{1/n} \frac{\tilde{\delta}}{I_n} \qquad \ldots(12)$$

for small values of $\tilde{u}_x$ we have:

$$d_n \approx \left(\frac{\alpha.\sigma_0}{E}\right)^{1/n} \left(\tilde{u}_y\right)^{1/n} \frac{2\tilde{u}_y}{I_n} \qquad \ldots(13)$$

Values of d_n from (Tracey, 1976) have been plotted in Figure A2 corresponding to plane strain. Hence from equ(11) the mode *I* stress intensity can be computed in a plastic strain field.

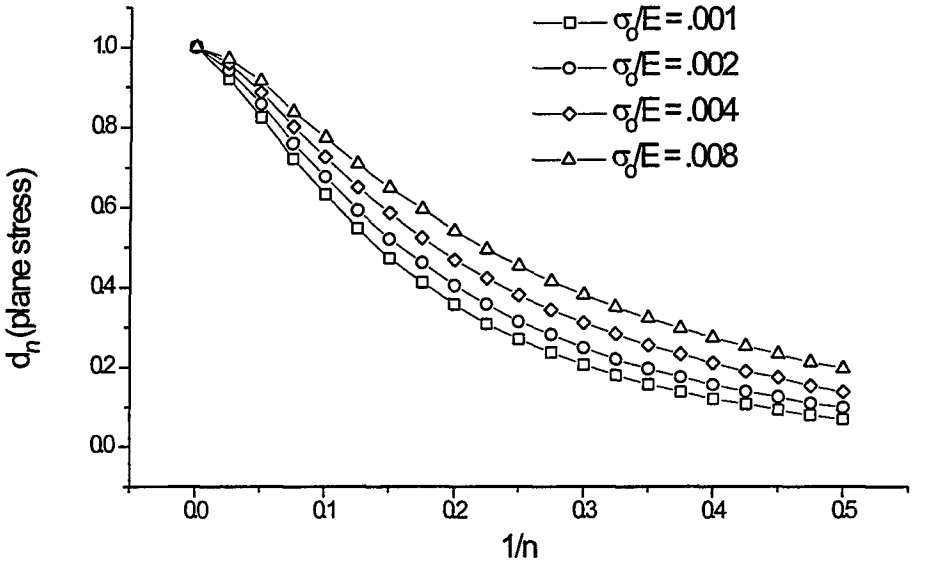

Figure A2. Values of d_n (Tracey, 1976) corresponding to plane strain

DISTRIBUTION LIST

Analysis of Fatigue Crack Growth from Cold-expanded/interference Fitted Stop Drilled Holes

R.J. Callinan, C.H. Wang and S. Sanderson

AUSTRALIA

DEFENCE ORGANISATION

S&T Program

Chief Defence Scientist
FAS Science Policy
AS Science Corporate Management
} shared copy

Director General Science Policy Development
Counsellor Defence Science, London (Doc Data Sheet)
Counsellor Defence Science, Washington (Doc Data Sheet)
Scientific Adviser to MRDC Thailand (Doc Data Sheet)
Director General Scientific Advisers and Trials/Scientific Adviser Policy and Command (shared copy)
Navy Scientific Adviser (Doc Data Sheet and distribution list only)
Scientific Adviser - Army (Doc Data Sheet and distribution list only)
Air Force Scientific Adviser
Director Trials

Aeronautical and Maritime Research Laboratory
Director

Chief of Airframes and Engines Division
Research Leader
Task Manager
R.J.Callinan,
C.H.Wang ,
S.Sanderson
M.Heller

DSTO Library
Library Fishermens Bend
Library Maribyrnong
Library Salisbury (2 copies)
Australian Archives
Library, MOD, Pyrmont (Doc Data sheet only)

Capability Development Division
Director General Maritime Development (Doc Data Sheet only)
Director General Land Development (Doc Data Sheet only)
Director General C3I Development (Doc Data Sheet only)

Army

ABCA Office, G-1-34, Russell Offices, Canberra (4 copies)

SO (Science), DJFHQ(L), MILPO Enoggera, Queensland 4051 (Doc Data Sheet only)

NAPOC QWG Engineer NBCD c/- DENGRS-A, HQ Engineer Centre Liverpool Military Area, NSW 2174 (Doc Data Sheet only)

Intelligence Program

DGSTA Defence Intelligence Organisation

Corporate Support Program (libraries)

OIC TRS, Defence Regional Library, Canberra

Officer in Charge, Document Exchange Centre (DEC) (Doc Data Sheet and distribution list only)

*US Defence Technical Information Center, 2 copies

*UK Defence Research Information Centre, 2 copies

*Canada Defence Scientific Information Service, 1 copy

*NZ Defence Information Centre, 1 copy

National Library of Australia, 1 copy

UNIVERSITIES AND COLLEGES

Australian Defence Force Academy

Library

Head of Aerospace and Mechanical Engineering

Deakin University, Serials Section (M list), Deakin University Library, Geelong, 3217

Senior Librarian, Hargrave Library, Monash University

Librarian, Flinders University

OTHER ORGANISATIONS

NASA (Canberra)

AGPS

OUTSIDE AUSTRALIA

ABSTRACTING AND INFORMATION ORGANISATIONS

INSPEC: Acquisitions Section Institution of Electrical Engineers

Library, Chemical Abstracts Reference Service

Engineering Societies Library, US

Materials Information, Cambridge Scientific Abstracts, US

Documents Librarian, The Center for Research Libraries, US

INFORMATION EXCHANGE AGREEMENT PARTNERS

Acquisitions Unit, Science Reference and Information Service, UK

Library - Exchange Desk, National Institute of Standards and Technology, US

SPARES (5 copies)

Total number of copies: **51**

DEFENCE SCIENCE AND TECHNOLOGY ORGANISATION
DOCUMENT CONTROL DATA

1. PRIVACY MARKING/CAVEAT (OF DOCUMENT)

2. TITLE

Analysis of Fatigue Crack Growth from Cold-expanded/interference Fitted Stop Drilled Holes

3. SECURITY CLASSIFICATION (FOR UNCLASSIFIED REPORTS THAT ARE LIMITED RELEASE USE (L) NEXT TO DOCUMENT CLASSIFICATION)

Document	U
Title	U
Abstract	U

4. AUTHOR(S)

R.J.Callinan, C.H.Wang and S.Sanderson

5. CORPORATE AUTHOR

Aeronautical and Maritime Research Laboratory
PO Box 4331
Melbourne Vic 3001

6a. DSTO NUMBER	6b. AR NUMBER	6c. TYPE OF REPORT	7. DOCUMENT DATE
DSTO-TR-0704	AR-010-604	Technical Report	July 1998

8. FILE NUMBER	9. TASK NUMBER	10. TASK SPONSOR	11. NO. OF PAGES	12. NO. OF REFERENCES
M1/9/510 1	95/140	DST	32	14

13. DOWNGRADING/DELIMITING INSTRUCTIONS

14. RELEASE AUTHORITY

Chief, Airframes and Engines Division

15. SECONDARY RELEASE STATEMENT OF THIS DOCUMENT

Approved for public release

OVERSEAS ENQUIRIES OUTSIDE STATED LIMITATIONS SHOULD BE REFERRED THROUGH DOCUMENT EXCHANGE CENTRE, DIS NETWORK OFFICE, DEPT OF DEFENCE, CAMPBELL PARK OFFICES, CANBERRA ACT 2600

16. DELIBERATE ANNOUNCEMENT

No Limitations

17. CASUAL ANNOUNCEMENT Yes

18. DEFTEST DESCRIPTORS

Finite Element Analysis, cracks, cold working, inserts

19. ABSTRACT

In this report a numerical study has been carried out into the fatigue life enhancement of a through cracked plate specimen using stop drilled holes at the end of each crack tip. Also the effect of cold working and the use of interference plugs are considered. While it has been found that under a static remote tension load the use of interference plugs gives no additional static strength, results from cyclic loads indicate that the accumulation of strain energy per cycle is less with interference fit plugs. Also the introduction of stationary cracks of crack-length *0.066* to *1.0mm* have been considered with constraints to prevent crack closure. The crack-tip opening displacements of re-initiated cracks at the edge of the stop hole have been determined using the finite element method, and it is found that the equivalent stress intensity factors are significantly higher than predicted by linear elastic fracture mechanics. Furthermore the use of these results together with the FASTRAN II computer program predicts fatigue lifetimes which are in reasonable agreement with experimental data.